Industrial Crops & Products 220 (2024) 119291

Contents lists available at ScienceDirect

Industrial Crops & Products

journal homepage: www.elsevier.com/locate/indcrop

# Application of $CaFe_2O_4/Ca_2Fe_2O_5$ to the fixation of heavy metals by co-combustion of coal and coconut shells: Experimental, simulation studies and environmental analysis

Zi You [a,b], Xiaoqian Ma [a,b,*], Zhaosheng Yu [a,b], Chunxiang Chen [c], Jinxi Dong [a,b], Wenchang Yue [a,b]

[a] School of Electric Power, South China University of Technology, Guangzhou 510640, China
[b] Guangdong Province Key Laboratory of Efficient and Clean Energy Utilization, Guangzhou 510640, China
[c] College of Mechanical Engineering, Guangxi University, University Road 100, Xixiangtang District, Nanning City 530004, China

ARTICLE INFO

*Keywords:*
Coal
Coconut shell
Heavy metals
Calcium-iron adsorbents
Ecological risk

ABSTRACT

The method of generating electricity by co-combusting coconut shells, a cash crop, with coal reduces emissions of gaseous pollutants from coal-fired power generation. Still, it tends to result in significant metal pollution. Two new calcium-iron type adsorbents, $CaFe_2O_4$ and $Ca_2Fe_2O_5$, were prepared in this study to reduce heavy metals in the atmosphere. Thermal adsorption experiments were carried out to study the fixation effect of $CaFe_2O_4$ and $Ca_2Fe_2O_5$ on six heavy metals, namely Cr, Cu, Mn, Ni, Pb, and Zn. The adsorbents were characterized by XRD, SEM, and BET, and the adsorption mechanism was investigated together with Factsage simulation. The study of the ecological risk of heavy metals showed that the heavy metals mixed in coal and coconut shells have a large $E_r$ (Ecological risk) value. When the two calcium-iron adsorbents were compared at the same mixing ratio, the $R_I$ (Risk index) value of $CaFe_2O_4$ was smaller than that of $Ca_2Fe_2O_5$. The results showed that $CaFe_2O_4$ and $Ca_2Fe_2O_5$ effectively fix six heavy metals by both physical and chemical adsorption. Among them, the optimum fixation (Cr, Cu, Mn, Ni, Pb, and Zn) of $CaFe_2O_4$ with different mixing ratios were increased by 27.75 %, 14.27 %, 10.51 %, 46.14 %, 17.69 %, and 10.66 % at 900 °C, respectively. In this study, two calcium-iron type adsorbents were prepared, experiments and simulations investigated their adsorption mechanisms, and their performances were comprehensively evaluated concerning the environmental risk factors, which opens a new way to reduce the emission of heavy metals in the co-combustion process of coal and biomass.

## 1. Introduction

Currently, combustion is the main route of fossil energy utilization, and heavy metals in coal are a significant source of pollution. In coal combustion, heavy metals are attached to the resulting fly ash and enter the atmosphere, and secondary pollution occurs with dry and wet precipitation (Wasielewski et al., 2021; Munawer, 2018; Luo et al., 2020). As a kind of clean energy with the advantages of being renewable, widely distributed, produced in large quantities, and inexpensive, biomass has become an alternative to coal, and the mixed combustion of coal and biomass has become the choice of many power plants. This type of combustion helps to effectively reduce greenhouse gas emissions (Saikaew et al., 2012).

The significant sources of pollution during combustion are heavy metal emissions, adsorption, condensation, and combustion methods, which are available to control heavy metals in flue gas. Among them, adsorbent control is an effective method to control heavy metal pollution due to the accessible collection of bottom ash and better adaptability (Ke et al., 2019). Current research is focused on searching for new heavy metal adsorbents or researching the modification of adsorbents, hoping to fix more heavy metals in the bottom ash to reduce atmospheric fugitive. Adsorbents can be divided into Ca-based, Al-based, and Si-based. Three types of adsorbents, such as metal oxides and many other mineral adsorbents, are the focus of researchers: kaolin (Yao and Naruse, 2009; Scotto et al., 1994), montmorillonite (Xue et al., 2021), limestone (Zhang et al., 2022), palygorskite (Wang et al., 2007), zeolite, dolomite, and seafoam (Zhao et al., 2018). Hu et al. have demonstrated that the mineral additive CaO can provide chemical sites for the

* Corresponding author at: School of Electric Power, South China University of Technology, Guangzhou 510640, China.
*E-mail address:* epxqma@scut.edu.cn (X. Ma).

https://doi.org/10.1016/j.indcrop.2024.119291
Received 7 March 2024; Received in revised form 23 June 2024; Accepted 19 July 2024
Available online 24 July 2024

adsorption of heavy metals, transforming them from toxic and unstable to non-toxic and stable states for harmless treatment (Hu et al., 2013). Zhang et al. investigated the behavior, morphology, and environmental risks of HMs (heavy metals: As, Cr, Zn, and Cu) during sludge combustion with the addition of CaO and montmorillonite (MMT) (Zhang et al., 2022). It was found that the addition of CaO inhibited the volatilization of Cr, Zn, and Cu and promoted the volatilization of As. In contrast, adding MMT inhibited As, Cr, Zn, and Cu volatilization, but "adsorption failure" appeared at high temperatures. Katarzyna Jagodzinska et al. investigated the adsorption of three adsorbents ammonium sulfate, kaolinite, and halloysite, at three dosages (2 %, 4 %, and 8 %) on bottom ash heavy metals (-oids). It was shown that ammonium sulfate fixed Cr, Cu, and Hg better, halloysite fixed Cd, Co, V, and Mn better, and kaolinite fixed Pb better (Jagodzińska et al., 2019).

In summary, adding metal oxide adsorbents can significantly increase the fixation rate of heavy metals. However, a single adsorbent has different selectivity for multiple heavy metals (Xue et al., 2021). Coal contains many types of heavy metals (Yao et al., 2004; Linak et al., 1995); therefore, adsorbents that can fix more heavy metals need further exploration. The calcium-iron type oxides $CaFe_2O_4$ and $Ca_2Fe_2O_5$ have the potential to be a new type of calcium-iron type heavy metal adsorbents, which have been used in previous studies in the fields of electrochemistry (Zhang et al., 2020), magnetism (Bo et al., 2021; Ueda et al., 2022), nanomaterials (Huang et al., 2021), photocatalytic degradation of environmental pollutants (Bouatam et al., 2022; Qomaruddin et al., 2020), and hydrogen production (Manohar et al., 2024), and have been demonstrated to have the ability to adsorb gaseous pollutants, such as CO, NO (Feng et al., 2020; Li et al., 2020). However, there are few studies on the effect and mechanism of heavy metal adsorption in combustion. Therefore, it is valuable to explore the addition of $CaFe_2O_4$ and $Ca_2Fe_2O_5$ additives in the blending process of coal and coconut shells to control heavy metal emissions. This study investigated the reaction pathways and fixation mechanisms by combining software simulations and experiments. At the same time, the environmental impact of adsorbent incorporation was concerned, and environmental risk factors comprehensively evaluated the performance of two calcium-iron type adsorbents.

In this paper, to reduce the pollution caused by heavy metals in the co-combustion process of coal and coconut shells, two calcium-iron type adsorbents are synthesized to fix heavy metals (Cr, Cu, Mn, Ni, Pb, Zn) in the bottom slag by using the adsorption of heavy metals in the coal and coconut shells fibers. The objective was to analyze the effect of heavy metal adsorbent addition on heavy metal content in slag by controlling the mixing ratio of heavy metal adsorbent and coal/biomass fuel. In addition, based on the experimental results, simulations were carried out using Factsage software to derive a mechanism model for heavy metal adsorption, which lays the foundation for exploring new heavy metal adsorbents. Meanwhile, the adsorption performance of two calcium-iron type adsorbents was comprehensively evaluated with environmental risk factors. This study innovatively explores using two calcium-iron type adsorbents, $CaFe_2O_4$ and $Ca_2Fe_2O_5$, in heavy metal fixation. It investigates the adsorption mechanism, which provides a solution to reduce the emission of heavy metals from the co-combustion of coal and biomass.

## 2. Experimental section

### 2.1. Materials

The coal used in this study was produced by Guangxi China Resources Power (Hezhou) Co. Ltd. and after grinding 80 mesh sieving and drying at 105°C for 24 hours, it was subjected to thermal experiments in a tube furnace. Coconut shells collected from vegetable markets in the Guangzhou area, were ground, sieved through an 80-mesh sieve, and dried at 105°C for 24 hours before being removed and set aside. A total of 1.25 g of coal and coconut shells were weighed in a ratio of 4:1 and mixed thoroughly.

The N, C, H, and S contents were determined using an elemental analysis for coal and coconut shells, respectively, and the O content was calculated. The results of the elemental and industrial analyses of coal and coconut shells are shown in Table S1 below. The results of the characterization of the composition of coal ash and coconut shell ash using an X-ray fluorescence spectrometer (XRF) are shown in Table S2 and Table S3. The heavy metal content (Cr, Cu, Mn, Ni, Pb, Zn) of coal and coconut shells is shown in Table S4.

### 2.2. Preparation of calcium-iron type adsorbents

$Ca(NO_3)_2{\cdot}4\ H_2O$ and $Fe(NO_3)_3{\cdot}9\ H_2O$ (AR analytical purity, ≥99 %) required for the experiments were purchased from the Guangzhou Chemical Reagent Factory. In this experiment, two calcium-iron adsorbents, $CaFe_2O_4$ and $Ca_2Fe_2O_5$, were prepared by the procedure of "precipitation-combustion-calcination" as follows:

$Ca(NO_3)_2{\cdot}4\ H_2O$ and $Fe(NO_3)_3{\cdot}9\ H_2O$ were dissolved in deionized water at a molar ratio of $n(Ca^{2+}):n(Fe^{3+})=1:2$ to obtain a mixed solution with a calcium ion concentration of 0.99 mol/L and a ferrous iron ion concentration of 1.98 mol/L. Then, at a molar ratio of n(urea):n $(Fe^{3+})$:1.4:1, a certain mass of urea was added to the above-mixed solution and heated and stirred under a water bath at 80°C until a sticky substance was formed. The resulting viscous material was placed in a muffle furnace, heated to 250°C in an air atmosphere at a 10 °C/min ramp rate and held for 30 minutes. Next, it was calcined at 900°C for 5 hours at a 15 °C/min rate. After cooling, the powder was ground and sieved through an 80-mesh sieve to obtain a calcium-iron adsorbent with $CaFe_2O_4$ as the main component.

$Ca(NO_3)_2{\cdot}4\ H_2O$ and $Fe(NO_3)_3{\cdot}9\ H_2O$ were dissolved in deionized water at a molar ratio of $n(Ca^{2+}):n(Fe^{3+})=1:1$ to obtain a mixed solution with both calcium ion concentration and iron ion concentration of 1.39 mol/L. Then, a certain mass of urea was weighed at a molar ratio of n(urea): $n(Fe^{3+})$ =2:1 and added to the above mix. The solution was heated and stirred at 70°C under a water bath until a sticky substance was formed. The resulting sticky substance was placed in a muffle furnace, heated to 250°C in an air atmosphere at an increasing rate of 5 °C/min, and held for 30 minutes. Next, it was calcined at 900°C for 5 hours at a 10 °C/min rate. After cooling, the powder was ground and sieved through an 80-mesh sieve to obtain a calcium-iron adsorbent with $Ca_2Fe_2O_5$ as the main component.

### 2.3. Experimental apparatus and methods

#### 2.3.1. Adsorption experiment

As shown in Fig.S1, combustion-adsorption experiments were carried out using a horizontal tube furnace. The schematic diagram of the experimental setup is shown below. The tube furnace was heated up to 900°C, and a 1 L/min flow rate of air was introduced into the tube using an air bottle. Then, the quartz boat containing the mixture of material (1.25 g of coal and coconut shells) was pushed into the tube for complete combustion, and the quartz boat was removed after 30 minutes to collect the bottom ash. In this, to investigate the adsorption effect of calcium-iron type adsorbents, $CaFe_2O_4$ and $Ca_2Fe_2O_5$ adsorbents with mass fractions of 3 %, 5 %, 10 %, and 20 % were added to the materials. After combustion, the collected ash was cooled and weighed. In addition, parallel experiments were conducted to ensure their accuracy.

#### 2.3.2. Analysis of experimental results

The collected bottom ash was poured into a PTFE beaker and moistened, and nitric acid, concentrated nitric acid, hydrogen peroxide, and hydrochloric acid were diluted and added to eliminate the solution. 40 mL of deionized water was added and boiled until 10 mL of solution remained. Finally, the beaker solution was filtered and volumetrically concentrated into a 25 mL volumetric flask. The resulting solution was fed into an ICP-OES (model 5100, Agilent Technologies Co. Ltd, Santa

Clara, CA, USA).

The process of processing the experimental data involved is shown in Eq. (1) and Eq. (2).

$$A = \frac{m_{ash}}{m_{fuel}} \times 100\% \quad (1)$$

Where the ash yields A: the mass of the fuel ash after the experiment as a mass fraction of the fuel before the experiment. $m_{fuel}$ is the mass of the fuel sample before the experiment, and mash is the mass of the ash after the experiment.

$$CE = \frac{C_{ash}}{C_{fuel}} \times A \times 100\% \quad (2)$$

Capture efficiency CE: The amount of heavy metals fixed in the bottom slag as a percentage of the mass fraction of heavy metals in the fuel is defined as the fixation rate of heavy metals. $C_{ash}$ content of heavy metals in the ash slag after the experiment, and $C_{fuel}$ the content of heavy metals in the fuel samples before the experiment, in mg/kg. A larger CE means a higher fixation rate.

The heavy metal products in the experiment were simulated and analyzed using Factsage 7.3. The software is based on the Gibbs minimum free energy method: the Gibbs free energy of the system is minimized under isothermal and isobaric conditions as an equilibrium criterion, and the Lagrange method of pending coefficients is used to solve for the composition and concentration of components at this time.

## 3. Results and discussion

### 3.1. Characterization of adsorbents

#### 3.1.1. Results of SEM and BET

As shown in Fig. 1, (a) and (b) show the surface structure of $CaFe_2O_4$. (c) and (d) show the surface structure of $Ca_2Fe_2O_5$. $CaFe_2O_4$ and $Ca_2Fe_2O_5$ were prepared using the "precipitation-combustion-calcination" procedure, in which many gases were released during the process, resulting in a porous structure. Due to the different synthesis parameters of the two adsorbents, their microscopic morphologies have significant differences. As seen in (a), the $CaFe_2O_4$ surface shows a spongy structure with a uniform distribution, similar to that of André Bloesser (Bloesser et al., 2020). This structure contributes to the fixation of heavy metals. Fig. 1(c) and (d), show that $Ca_2Fe_2O_5$ has a chain-like structure, and the particles are interconnected to form a porous structure (Benallal et al., 2022). Table 1 demonstrates the pore characteristics of limestone and $CaFe_2O_4$ with $Ca_2Fe_2O_5$ from Zheng et al. (Zheng et al., 2017). It can be found that $CaFe_2O_4$ and $Ca_2Fe_2O_5$ have a larger specific surface area than limestone, a typical heavy metal adsorbent. In terms of the average pore diameter of the specific surface area, $CaFe_2O_4$ is larger than $Ca_2Fe_2O_5$. Increasing the particular surface area, pore volume, and pore diameter is conducive to providing more space for physical adsorption (Yang et al., 2023a), which favors the physical adsorption of heavy metals from fly ash. In addition, it also facilitates the exhibition of more active sites, which is also favorable for chemical adsorption.

#### 3.1.2. Results of XRD

To investigate the chemical composition and crystalline structure of the two calcium-iron type adsorbents prepared at 900 °C, they were characterized by XRD. The results of XRD characterization of $CaFe_2O_4$ and $Ca_2Fe_2O_5$ are shown in Fig. 2(a) and (b).It can be seen that the characteristic peaks of $CaFe_2O_4$ appear near 2θ = 19.2°, 25.4°, 33.6°, 35.4°, 40.2°, 42.7°, 46.2°, 49.6°, 61.2°, and 71.6° in the diffraction peak curves of $CaFe_2O_4$, (Zhang et al., 2020) This proves that $CaFe_2O_4$, has been successfully prepared by the "precipitation-combustion-calcination" procedure; however, due to the addition of $Ca(NO_3)_2{\cdot}4\ H_2O$ and $Fe(NO_3)_3{\cdot}9\ H_2O$ during the preparation, small amounts of $Fe_2O_3$ and $Ca(OH)_2$ were detected in the samples. heterogeneous peaks.

Similarly, the diffraction peak profiles of $Ca_2Fe_2O_5$ demonstrate that the "precipitation-combustion-calcination" procedure has successfully prepared $Ca_2Fe_2O_5$, and peaks of $Fe_2O_3$ are detected at 2θ = 23°, 33°,

Table 1
Pore characteristics of $CaFe_2O_4$ and $Ca_2Fe_2O_5$.

| Material | Specific Surface Area ($m^2/g$) | Pore Volume ($cm^3/g$) | Mean Pore Size (nm) |
|---|---|---|---|
| Natural limestone (Zheng et al., 2017) | 0.63 | 1.74E−04 | 11.11 |
| $CaFe_2O_4$ | 3.88 | 1.56E−02 | 16.14 |
| $Ca_2Fe_2O_5$ | 2.17 | 7.95E−03 | 14.67 |

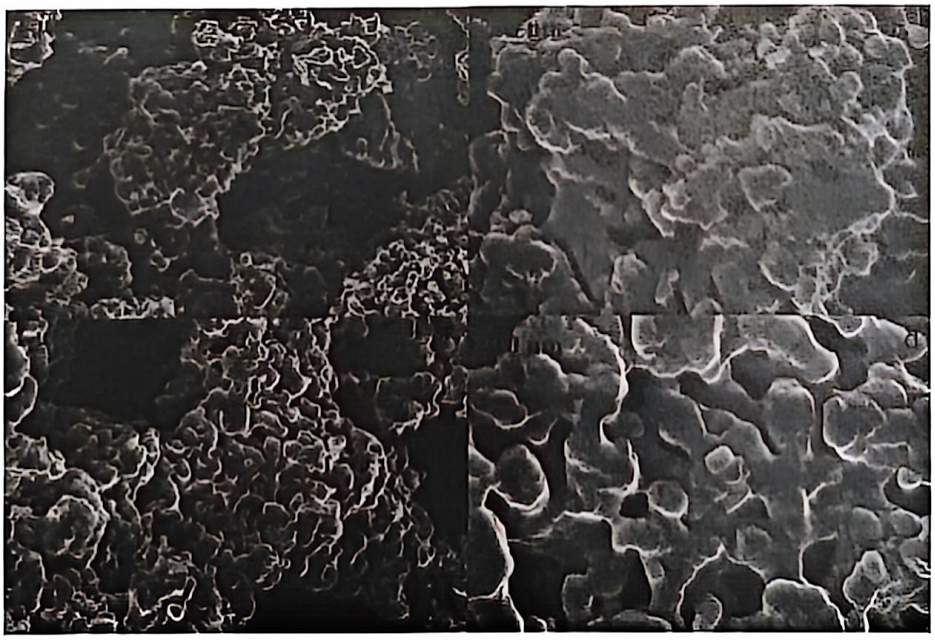

Fig. 1. SEM scans of (a), (b) $CaFe_2O_4$ and (c), (d) $Ca_2Fe_2O_5$.

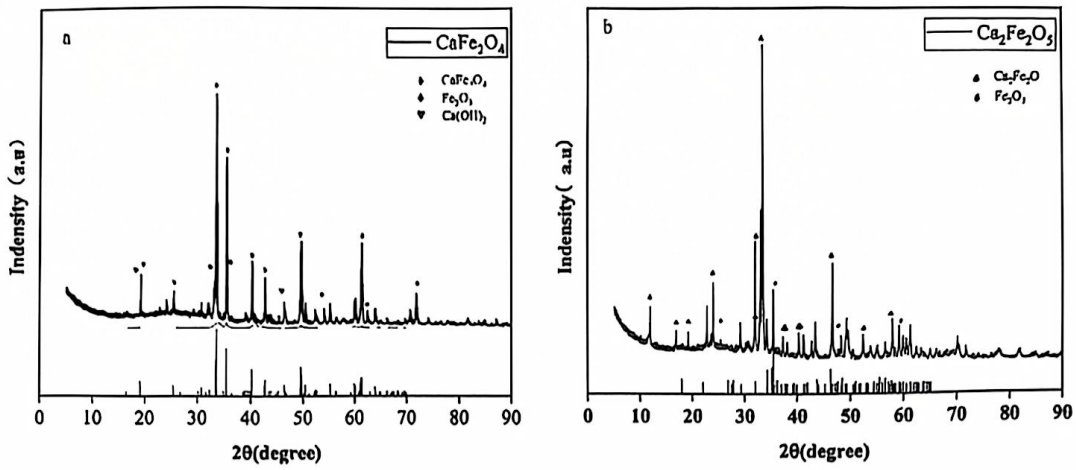


Fig. 2. XRD results of (a) $CaFe_2O_4$ and (b) $Ca_2Fe_2O_5$.

and 62°, which can be regarded as a by-product of the preparation method.

### 3.2. Fixation of heavy metals by calcium-iron type adsorbents

Fig. 3 shows the effect of two calcium-iron type adsorbents on the fixation of Cr, Cu, Mn, Ni, Pb, and Zn heavy metal elements in the co-combustion of coal and coconut shells. The larger the CE, the better the fixation is considered to be. The adsorbent was considered functional when the CE values derived from the different mixing ratios were higher than the CE values of coal and coconut shells without added adsorbent. Table 2 shows the products on Cr, Cu, Mn, Ni, Pb, and Zn for six heavy

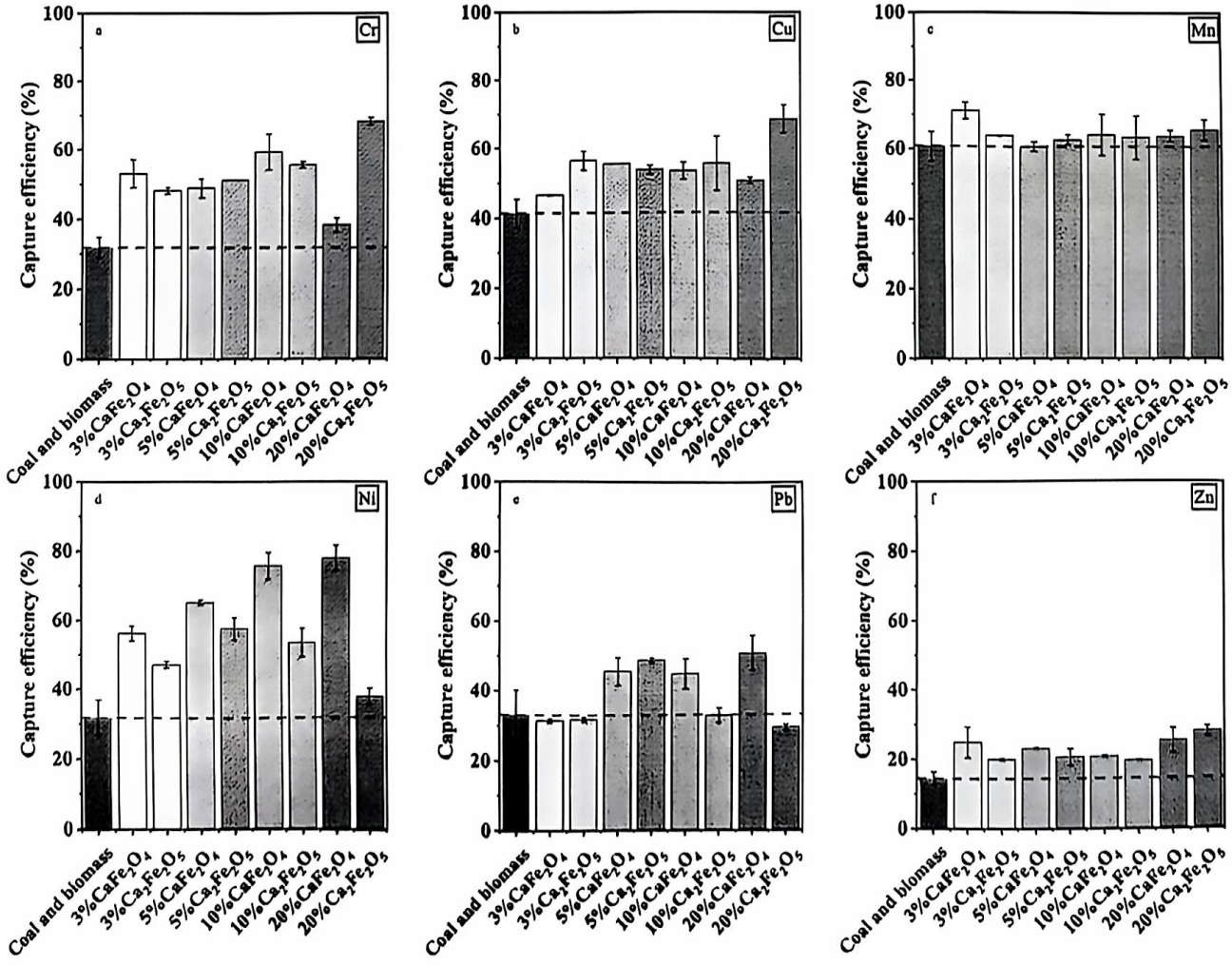


Fig. 3. Fixation rate of heavy metals by two calcium-iron type adsorbents.

Table 2
Heavy metal products calculated using FactSage 7.3.

| Additives | Heavy metals | Gaseous products | Solid products |
|---|---|---|---|
| $CaFe_2O_4$ | Cr | $CrO_2(OH)_2$ | $FeCr_2O_4$、$Cr_2O_3$ |
| | Cu | CuCl | · |
| | Mn | $MnCl_2$ | $Mn_2O_3$ |
| | Ni | $Ni(OH)_2$、$NiCl_2$ | $AlNi_2O_4$、$FeNi_2O_4$、$MgNi_2O_4$ |
| | Pb | PbO、$PbCl_2$ | $Pb_2Al_2O_7$、$Pb_2AlSi_2O_7$、$Pb_2FeAl_2O_7$、$Pb_2FeSi_2O_7$、$Pb_2AlFe_2O_7$ |
| | Zn | $ZnCl_2$ | $ZnFe_2O_4$、$ZnAl_2O_4$、$ZnNi_2O_4$ $Ca_2ZnSi_2O_7$、$Ca_2ZnAl_2O_7$ |
| $Ca_2Fe_2O_5$ | Cr | $CrO_2(OH)_2$ | $CaCr_2O_4$、$Cr_2O_3$ |
| | Cu | CuCl | · |
| | Mn | $MnCl_2$ | $Mn_2O_3$ |
| | Ni | $Ni(OH)_2$、$NiCl_2$ | $AlNi_2O_4$、$FeNi_2O_4$、$MgNi_2O_4$ |
| | Pb | PbO、$PbCl_2$ | $Pb_2FeAl_2O_7$、$Pb_2FeSi_2O_7$、$Pb_2AlFe_2O_7$ |
| | Zn | $ZnCl_2$ | $ZnFe_2O_4$、$ZnAl_2O_4$、$Ca_2ZnSi_2O_7$、$Ca_2ZnAl_2O_7$ |

metals based on Fastage7.3 software for coal and coconut shells co-combustion with the addition of two metal oxide adsorbents, $CaFe_2O_4$ and $Ca_2Fe_2O_5$, respectively.

### 3.2.1. Cr

For Cr, the gaseous product is mainly $CrO_2(OH)_2$ containing Cr6+, and the volatilization rate of Cr6+ is high at high temperatures (Gong et al., 2021). The incorporation of $CaFe_2O_4$ and $Ca_2Fe_2O_5$ at different mixing ratios significantly increased the fixation rate, with the best results for $CaFe_2O_4$ at 10 % mixing and $Ca_2Fe_2O_5$ at 20 % mixing, which proved that the adsorbent was effective for Cr. Interestingly, it can be seen from Table 2 that the solid products after the addition of $CaFe_2O_4$ are $FeCr_2O_4$ and $Cr_2O_3$, while the products after the addition of $Ca_2Fe_2O_5$ are $CaCr_2O_4$ and $Cr_2O_3$. The product difference explains why the two adsorbents have different fixation effects on Cr. The relevant reaction equations are given below. By calculation, the Gibbs free energies of all three reactions are less than 0, which means that the following responses for fixing chromium can proceed spontaneously.

$CaCr_2O_4$ is a new product produced by adding $CaFe_2O_4$ and $Ca_2Fe_2O_5$, which helps stabilize Cr. The exact product-related mechanism emerged from studies of calcium-based adsorbents (Gong et al., 2021), confirming the possibility of **reactions (3) and (5)**. The provision of more $Fe_2O_3$ by the addition of $CaFe_2O_4$ triggers the following **reaction (4)**, which ultimately fixes Cr in the bottom ash in the form of $FeCr_2O_4$. As $Ca_2Fe_2O_5$ provides less $Fe_2O_3$, the primary **reaction (5)** takes place, ultimately fixing Cr in the bottom ash in $CaCr_2O_4$. It should also be noted that both $FeCr_2O_4$ and $Cr_2O_3$ are Cr3+, which is less toxic than Cr6+ (Kenfoud et al., 2020).

$$2CaFe_2O_4 + 4CrO_2(OH)_2 = 2CaCr_2O_4 + 2Fe_2O_3 + 3O_2 + 4H_2O\ (\Delta G=-370346.4) \quad (3)$$

$$Fe_2O_3 + 4CrO_2(OH)_2 = 2FeCr_2O_4 + 3.5H_2\ (\Delta G=-317611.1) \quad (4)$$

$$Ca_2Fe_2O_5 + 4CrO_2(OH)_2 = 2CaCr_2O_4 + Fe_2O_3 + 3O_2 + 4H_2O\ (\Delta G=-375812.0) \quad (5)$$

### 3.2.2. Cu

From the effects of the two ads, Cu is a volatile metal, and the fixation rate of Cu at 900 °C was low due to the increase in Cu's volatility with the temperature rise. Adding two adsorbents, $CaFe_2O_4$ and $Ca_2Fe_2O_5$, improved the adsorption rate by 8–30 %, which is a significant improvement. FactSage calculations showed that the main products of $CaFe_2O_4$ and $Ca_2Fe_2O_5$ were the same, and CuCl dominated the gaseous products. This is due to the presence of Cl in coal, which combines with heavy metals to form chlorides and contributes significantly to flaring (Zhu et al., 2024). The fixed product of Cu may be $Cu_2O$ (Chen et al., 2019). Solid products were not represented due to the discrepancy between software simulations and complex actual combustion and the inability to simulate the effect of physical adsorption. $CaFe_2O_4$ and $Ca_2Fe_2O_5$ are reducing in nature. According to Chen's results, the fixation of Cu by calcium-iron adsorbents may be partly due to physical and chemical adsorption of part of the $CuCl_2$ converted to $Cu_2O$. Sorbents, $CaFe_2O_4$, and $Ca_2Fe_2O_5$, showed better adsorption effects in 3 % and 20 % mixing ratios. The effects of the two adsorbents did not differ much in the 5 % and 10 % intermediate mixing ratios. Notably, both adsorbents have higher fixation rates than coal and coconut shells without adsorbents.

### 3.2.3. Mn

Mn is a low-volatile heavy metal that tends to melt and form agglomerates at high temperatures (900°C), which helps enhance the ash's structural stability. The experimental results are shown in Fig. 3, where the Mn fixation rate can reach 60 % even without adding adsorbent. During combustion, the volatilized Mn was mainly attached to the fly ash and discharged with it (Jagodzińska et al., 2019).

Adding two adsorbents, $CaFe_2O_4$ and $Ca_2Fe_2O_5$, resulted in a slight increase in the Mn fixation rate. The gaseous products after the simulation were mainly $MnCl_2$, and the molar amounts of the relevant reactions were small, which also agreed with the experimental results. Most of the products were concentrated in the solid product $Mn_2O_3$. $CaFe_2O_4$ has the best Mn-fixing effect at an addition of 3 %, and there is no significant change in the other additions. Due to the low oxidation of $CaFe_2O_4$ and $Ca_2Fe_2O_5$ (Miller and Siriwardane, 2018), the chemisorption effect between the adsorbent and Mn was not noticeable. Still, the physical adsorption of the surface structure was mainly used to reduce the generation of fly ash, which was also consistent with the results of BET characterization. Therefore, the adsorption effect of $CaFe_2O_4$ was slightly better than that of $Ca_2Fe_2O_5$.

### 3.2.4. Ni

Ni is a non-volatile element at 900°C (Oboirien et al., 2016). According to the experimental results in Fig. 3, it was found that the Ni fixation rate was low when coal and coconut shells were mixed and combusted. However, adding two adsorbents, $CaFe_2O_4$ and $Ca_2Fe_2O_5$, significantly improved the Ni fixation rate compared to the case without adsorbents. Combining the experimental results with simulations, the main gaseous products associated with Ni were $Ni(OH)_2$ and $NiCl_2$, and the solid products included $AlNi_2O_4$, $MgNi_2O_4$, $FeNi_2O_4$, and $NiFe_2O_4$, with a higher content of $FeNi_2O_4$. This is consistent with the results of (Chen et al., 2019). Combining the reactants and products derived from experiments and simulations, **reactions (6), (7), and (8)** are related to the addition of $CaFe_2O_4$, and their Gibbs free energy is below 0, indicating that these reactions can occur. These reactions suggest that the addition of calcium-iron type adsorbents $CaFe_2O_4$ and $Ca_2Fe_2O_5$ is favorable to increase the content of $NiFe_2O_4$, which explains the increase in the fixation rate of Ni. Meanwhile, the Gibbs free energy of reaction **(9)** is greater than 0, indicating that this reaction is unlikely to occur. Therefore, $CaFe_2O_4$ has the advantage of reacting directly with Ni-related gaseous products compared to $Ca_2Fe_2O_5$, which explains why the fixation rate of $CaFe_2O_4$ is superior to that of $Ca_2Fe_2O_5$ in Fig. 3.

The adsorbent $CaFe_2O_4$ increased Ni's fixation rate with the added amount's increase, reaching the maximum at 20 %. Meanwhile, $Ca_2Fe_2O_5$ reached the highest at 5 %. Comparing the effects of the two adsorbents at the same mixing ratio, the fixation rate of $CaFe_2O_4$ was generally higher than that of $Ca_2Fe_2O_5$, which indicated that $CaFe_2O_4$ had a better fixation effect in the fixation of Ni.

$$NiCl_2 + CaFe_2O_4 = NiFe_2O_4 + CaCl_2(\Delta G\rightarrow -90617.8) \quad (6)$$

$$Ni(OH)_2 + Fe_2O_3 = NiFe_2O_4 + H_2O\ (\Delta G \rightarrow -128511.0) \quad (7)$$

$$Ni(OH)_2 + CaFe_2O_4 = NiFe_2O_4 + Ca(OH)_2\ (\Delta G \rightarrow -49667.7) \quad (8)$$

$$Ni(OH)_2 + Ca_2Fe_2O_5 + H_2O = NiFe_2O_4 + 2Ca(OH)_2\ (\Delta G \rightarrow 23710.0) \quad (9)$$

### 3.2.5. Pb

Pb is a toxic heavy metal that can cause more significant environmental harm, and adding adsorbents can effectively reduce its environmental hazards (Singh et al., 2018). Coal and coconut shells contain more Pb, which has a $C_{fuel}$ (mg/kg) of 20.4 mg/kg and is mainly present in coal. Pb is a volatile trace-heavy element in coal. As seen in Fig. 3, pure coal with coconut shells combustion only had about 36 % fixation of Pb. This is due to the higher $K_2O$ of coconut shells as biomass. Incorporating higher K compounds promotes the melting of ash, which disrupts the aluminosilicate structure and ultimately releases residual Pb. Fortunately, Pb can be effectively contained in the bottom ash after increasing the mixing ratio after calcium-iron type adsorbents. Among them, $Ca_2Fe_2O_5$ can achieve more than 50 % fixation rate at 5 % and 20 % mixing ratios. The main products of Pb are $PbCl_2$, and the solid products are $Pb_2Al_3O_7$, $Pb_2AlSi_2O_7$, $Pb_2FeAl_2O_7$, $Pb_2FeSi_2O_7$, $Pb_2AlFe_3O_7$.

The two adsorbents, $CaFe_2O_4$ and $Ca_2Fe_2O_5$, showed a volatilization-promoting effect on Pb at a small addition amount (3 %). This may be because the primary **reaction (10)** occurs at relatively low additions and spontaneously reacts with $PbSO_4$ to produce a more gaseous product, $PbCl_2$. Based on Chen's theory of calcium-based adsorbents, in the absence of calcium-based adsorbents, HCl cannot respond with $PbSO_4$ to form $PbCl_2$ (g), and the solid product $PbSO_4$ cannot be converted to a gaseous product, which explains why the volatilization efficiency of Pb was improved at 3 % additions and also proves the reliability of the reaction (Chen et al., 2019). Meanwhile, with the increase of the addition amount, the two adsorbents, $CaFe_2O_4$ and $Ca_2Fe_2O_5$, showed a fixation effect on Pb. In comparing the two adsorbents, the fixation effect of $CaFe_2O_4$ was slightly inferior to that of $Ca_2Fe_2O_5$ at low and medium additions (5 %). At temperatures greater than 900 °C, the gaseous product is mainly in the form of PbO (Lai et al., 2020), which reacts with two calcium-iron type adsorbents **reactions (11)** and **(12)** (the software was unable to calculate the free energies due to the lack of data on $Pb_2Al_3O_7$), which is also similar to Lai's results (Lai et al., 2020). One of them, $CaFe_2O_4$, can react with $Pb_2Al_3O_7$, reducing the amount of $Pb_2Al_3O_7$, which, according to Le Chatelier's principle, leads to a positive progression of the **reaction 11**, thus the fixation of Pb.

$$PbSO_4 + CaCl_2 = PbCl_2 + CaSO_4\ (\Delta G = -73615.4) \quad (10)$$

$$PbO + 6Al_2O_3 + O_2 = 4Pb_2Al_3O_7 \quad (11)$$

$$Pb_2Al_3O_7 + CaFe_2O_4 = Pb_2FeAl_2O_7 + CaO + Al_2O_3 \quad (12)$$

### 3.2.6. Zn

Zn and Pb have similar volatilization characteristics. The temperature has the greatest effect on Zn and Pb. The volatilization rates of Zn and Pb at 900 °C are 1.5 ~ 3.5 times higher than at 700 °C (Jagodzińska et al., 2019). This is the reason why the fixation rate of Zn was only slightly enhanced by both adsorbents, $CaFe_2O_4$ and $Ca_2Fe_2O_5$, without the addition of the adsorbent and the experimental group with the addition of the adsorbent compared to the other heavy metals. The Zn fixation rate was only 18 % for the combustion of pure coal and coconut shells. Combined with the experimental results, the gaseous product associated with Zn was calculated to be $ZnCl_2$, and the solid products were $ZnFe_2O_4$, $ZnAl_2O_4$, $ZnNi_2O_4$, $Ca_2ZnSi_2O_7$, and $Ca_2ZnAl_2O_7$. However, $ZnAl_2O_4$ also readily decomposed at high temperatures to volatilize as Zn. The trapping of Zn is mainly associated with the formation of $ZnO\text{-}Fe_2O_3$ complexes (Jagodzińska et al., 2019), which, in conjunction with the experiments, in which $ZnFe_2O_4$ may be a product of the addition of elevated $CaFe_2O_4$ and $Ca_2Fe_2O_5$. Previous studies have shown that the effect of Zn volatilization efficiency is mainly in the reaction with HCl and heavy metal chlorides (Chen et al., 2019), as shown in **reactions (13) and (14)**. The ΔG of both reactions is less than 0. The reactions are spontaneous and block the binding of Zn to Cl, thus increasing the fixation (Ran et al., 2019). However, comparative results show that the absolute value of ΔG for **reaction (13)** is relatively small. In contrast, the HCl limits the extent of **reaction (14)** in the flue gas, which limits both reactions and explains why there is an enhancement of Zn by adding both calcium-iron type adsorbents, but the overall CE is small.

$CaFe_2O_4$ with 3 % and 20 % additions showed better fixation. Combined with the results of the BET characterization, this can be attributed to the fact that the specific surface area and pore size of $CaFe_2O_4$ are better than those of $Ca_2Fe_2O$, and therefore, it can be concluded that it is due to the enhancement of physical adsorption that the calcium-iron adsorbent, $CaFe_2O_4$, adsorbs Zn better than $Ca_2Fe_2O_5$.

$$ZnCl_2 + CaFe_2O_4 = ZnFe_2O_4 + CaCl_2\ (\Delta G = -50997.5) \quad (13)$$

$$ZnCl_2 + Ca_2Fe_2O_5 + 2HCl = ZnFe_2O_4 + 2CaCl_2 + H_2O\ (\Delta G = -109721.7) \quad (14)$$

In summary, calcium-iron type adsorbents can effectively fix heavy metals and reduce heavy metal pollution during the co-combustion of coconut shells. Compared with common adsorbents in other studies (Chen et al., 2019; Yang et al., 2023b), their adsorption effects on typical heavy metals are shown in Table S5 of the Supplementary Material. In addition, thermal stability and cycling performance studies were carried out to explore the suitability of calcium-iron type adsorbents, as detailed in **Fig.S2 and S3** of the Supplementary Material.

## 3.3. Net fixation efficiency of heavy metals by calcium-iron type adsorbents

The heavy metal adsorption test goes through the adsorption and elimination tests. During these two processes, the test results are affected by various aspects, such as the fixation of heavy metals attached to the tube during the combustion process, the heavy metals that may be brought in during the elimination process, and the heavy metals contained in the adsorbent.

Therefore, to provide a more objective and intuitive response to the fixation effect of the adsorbent, a novel calculation method will be adopted in this paper. The following **calculation** Eq. (15) defines the net fixation efficiency parameter Δ.

$$\Delta = CE_{add} - CE_{without} \quad (15)$$

$CE_{add}$ denotes the heavy metal fixation rate obtained by combusting coal and coconut shell samples mixed with two calcium-iron type adsorbents in a tube furnace, and the resulting ash mixed with adsorbent, coal, and biomass was digested and measured by ICP. $CE_{without}$ denotes the heavy metal fixation rate obtained by combusting the ash obtained by combusting coal and coconut shell samples in a tube furnace, and the ash obtained by adding two calcium-iron type adsorbents with the corresponding mixing ratios was digested together with the adsorbent and measured by ICP. The heavy metal fixation rates were calculated by ICP after the coal and coconut shell blended ashes were decarburized with the sorbent by adding two types of calcium-iron sorbents with corresponding mixing ratios. Subtracting $CE_{add}$ and $CE_{without}$ gives the net fixation efficiency parameter Δ, which represents the additional heavy metals fixed in the coal and coconut shell samples due to the addition of the sorbents to the co-combustion. A larger Δ indicates better fixation. Fig. 4 shows the net adsorption efficiency of each heavy metal.

For Cr and Cu, comparing Fig. 3 and Fig. 4, the trends in fixation rates and net fixation efficiency are the same. The value of Δ was always

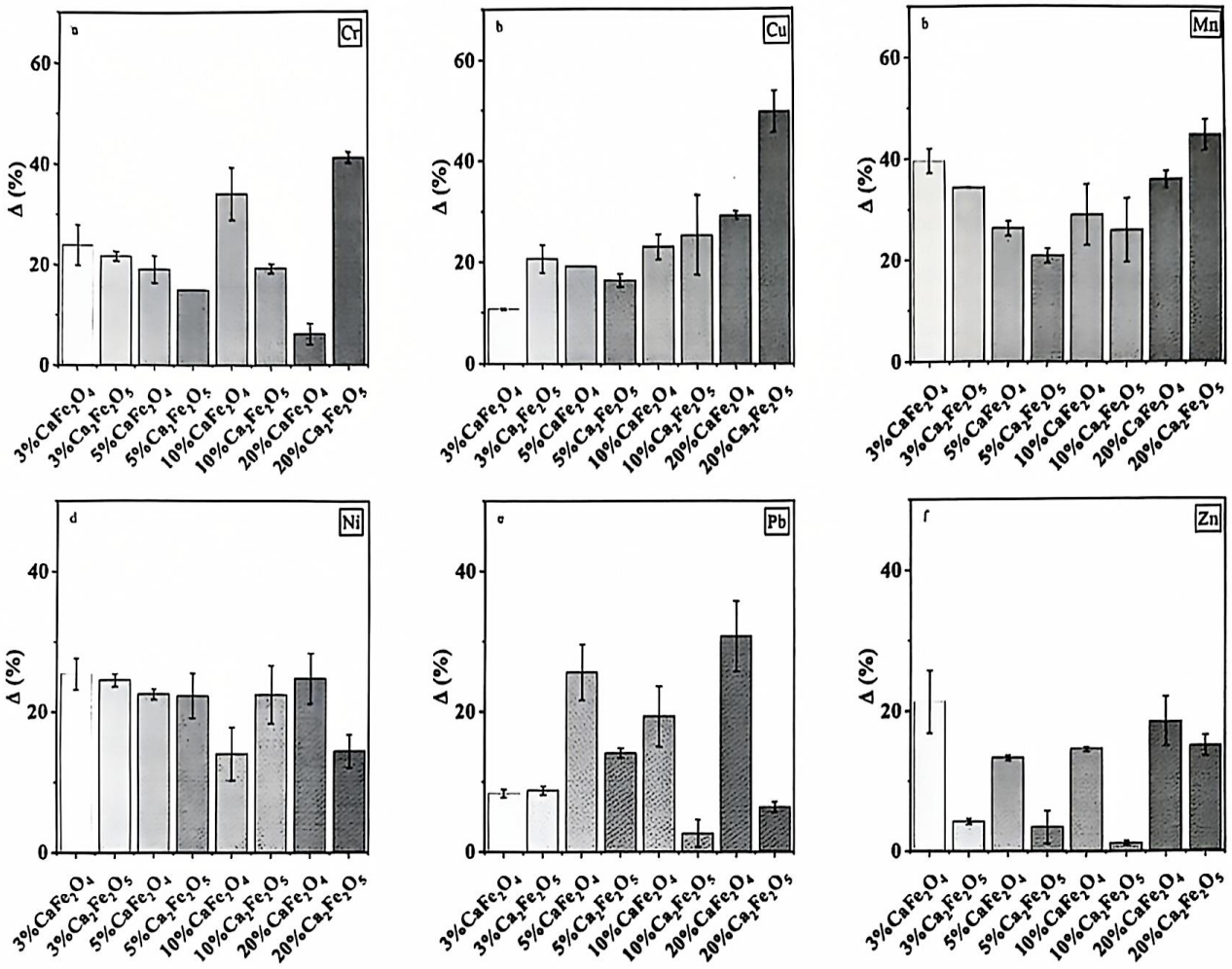


Fig. 4. Net fixation efficiency of heavy metals by two calcium-iron type adsorbents.

greater than 0 at different mixing ratios, demonstrating the significant fixation of Cr by $CaFe_2O_4$ and $Ca_2Fe_2O_5$. For $CaFe_2O_4$, the highest net fixation efficiency was achieved at a 10 % mixing ratio, consistent with the adsorption efficiency CE. Similarly, $Ca_2Fe_2O_5$ achieved the highest net fixation efficiency at 20 % mixing ratio, which is also consistent with CE and further validates the reliability of CE. Comparing the two calcium-iron type adsorbents, it is found that, in agreement with CE, $CaFe_2O_4$ is more effective than $Ca_2Fe_2O_5$ at 3 % and 10 % mixing ratios, and $Ca_2Fe_2O_5$ is superior at large mixing amounts. As for Cu, it can be noticed that Δ tends to increase with adsorbent admixture, which means that the fixation produced due to adsorbent incorporation is improving. This is because adding more adsorbents favors the production of more $Cu_2O$, which fixes Cu in the bottom ash. It can also be assumed that the adsorption effect of $CaFe_2O_4$ and $Ca_2Fe_2O_5$ on Cu mainly comes from chemisorption. Comparing the two adsorbents $CaFe_2O_4$ and $Ca_2Fe_2O_5$, although the adsorption efficiencies of the two adsorbents are almost the same in the intermediate mixing ratios of 5 % and 10 % from the CE point of view, from the point of view of Δ, the mixing ratio of 5 % $CaFe_2O_4$ is higher than that of the same ratio of $Ca_2Fe_2O_5$, which implies that the effect of $CaFe_2O_4$ will be improved more after adding $CaFe_2O_4$ in this ratio is more excellent. Combining the CE and Δ indexes, the adsorption effect of $Ca_2Fe_2O_5$ on Cu is more amazing.

Regarding Mn and Ni, CE and Δ show a slight difference. From Fig. 3, it is found that the CE value of Mn is only slightly increased after the addition of two adsorbents, $CaFe_2O_4$ and $Ca_2Fe_2O_5$. However, the difference in the adsorption effect brought about by adding adsorbents can be seen from the Δ plot. The Δ value of $CaFe_2O_4$ is higher at the low and medium mixing ratios of 3 %, 5 %, and 10 %. It means that $CaFe_2O_4$ has a better synergistic effect with coal and coconut shell blending than $Ca_2Fe_2O_5$ when errors such as heavy metals that may be contained in the adsorbent are subtracted. Although there has been an increase in incorporation, the increase has been slight, about 5 %, and the Δ value decreases as the blending amount rises, which is also consistent with the CE results. At 20 % mixing ratio, $Ca_2Fe_2O_5$ shows a better fixation rate. The Δ plot of Ni in Fig. 4 indicates that there is a net addition of 15–30 % with the addition of the two calcium-iron type adsorbents, implying a more significant enhancement of the co-combustion compared to coal and biomass without the addition of adsorbents. This is also consistent with the CE results. Comparing the Δ plots, the increase in the degree of mixing did not improve the net fixation efficiency, which reached a minimum at 10 % mixing rate. This is contrary to the results of CE, which showed the highest fixation rate of $CaFe_2O_4$, 10 % mixing amount. This may be because some Ni was introduced into the $CaFe_2O_4$ samples during preparation, slightly increasing Ni data after digestion. The Δ value of $Ca_2Fe_2O_5$ showed the same pattern as that of CE, and this result proved that there was no excess Ni introduced into $Ca_2Fe_2O_5$, and the CE results and Δ also corroborated each other to confirm the adsorption effect of $Ca_2Fe_2O_5$ for Ni. Combining the two indexes of CE and Δ, $CaFe_2O_4$ is generally better than $Ca_2Fe_2O_5$ in the same mixing ratio.

As shown in Fig. 4, the net fixation efficiency enhancement of both calcium-iron type adsorbents for Pb is weak at a low mixing rate of 3 %.

The net fixation efficiency of $CaFe_2O_4$ increased with increasing mixing ratios and was at its maximum at 5 % and 20 % mixing ratios, which are also similar to the results of CE. 5 % $Ca_2Fe_2O_5$ reached the best effect and started to decrease at 10 %. For Zn, in the Δ index, it can be found that the fixation rate of Zn after the addition of $CaFe_2O_4$ and $Ca_2Fe_2O_5$ is slightly increased, which is consistent with the results of CE. The fixation rate of $CaFe_2O_4$ is highest at a low mixing level of 3 %, then decreases with the increase of the mixing level, and then elevates again at a mixing ratio of 20 %. For $Ca_2Fe_2O_5$, the pattern is similar to $CaFe_2O_4$, but the adsorption effect is not as apparent as $CaFe_2O_4$.

### 3.4. Ecological risk of heavy metals

In coal-fired power plants, heavy metals are discharged into the environment with fly ash, which poses a significant risk to the ecological environment (Hu et al., 2021). To compare the adsorption effect of the two calcium-iron type adsorbents more objectively, their impact on the ecological risk to the environment will be considered. According to Chen's study, the ecological risk factor and risk index will be considered. Among them, the ecological risk factor $E_r$ is defined as each heavy metal volatilized into the gas; the risk index $R_I$ is used to characterize the degree of heavy metal pollution (Chen et al., 2019).

$$E_r = T_r \frac{C_i}{C_r} \tag{16}$$

$$R_I = \sum E_r \tag{17}$$

In Calculation (16), $E_r$ is the single potential ecological risk factor for gaseous heavy metals; Tr is the heavy metal toxicity response factor, $C_i$ (μg/m$^3$) is the measured concentration of heavy metals, and $C_r$ (μg/m$^3$) is the concentration of heavy metals in the atmosphere. In Calculation (17), $R_I$ is the sum of the respective heavy metal ecological risk factors. The gas volume for this experiment was 0.03 m$^3$.

According to Lars Hakanson, the heavy metal toxicity response factors and the atmospheric concentrations of heavy metals are shown in Table 3 (Hakanson, 1980; Zhuang and Lu, 2020). Calculated by Calculation (16) and (17).

By calculating, the results are shown in Table 4. The $E_r$ of each heavy metal shows that the $E_r$ values of heavy metals are high. It shows that, without any tail gas treatment measures, if the coal-fired power plant mixes the coal with coconut shells for combustion, the heavy metals discharged into the atmosphere and fly ash will significantly impact the environment.

Combined with $E_r$ and $R_I$, the $E_r$ and overall $R_I$ of each heavy metal decreased significantly after the addition of calcium-iron type adsorbents, which proved that $CaFe_2O_4$ and $Ca_2Fe_2O_5$ had a noticeable effect on the reduction of environmental pollution caused by the spillover of the heavy metals in coal. The pattern of change of $E_r$ and the fixation rate of the heavy metals, CE, had the same pattern of change. Among them, Cu, Ni, and Pb toxicity is higher, but the Er value of Pb is relatively tiny because Pb is also present in higher atmospheric concentrations. The volatility of Ni is more significant, and the toxicity is high, which creates a relatively substantial risk.

Fig. 5 illustrates the variation and trend of $E_r$ for coal and coconut shells blended with adsorbents. Cr has a high potential ecological risk.

Table 3
Heavy metal concentrations in the atmosphere.

| Area | Heavy metal | $T_r$ | $C_r$(ng/m$^3$) |
|---|---|---|---|
| South China | Cr | 2 | 31.7 |
| | Cu | 5 | 55.3 |
| | Mn | 1 | 25.3 |
| | Ni | 5 | 6.4 |
| | Pb | 5 | 277.1 |
| | Zn | 1 | 504.1 |

Its concentration in the atmosphere is very low, only higher than Ni, and $CaFe_2O_4$ at a 10 % blending ratio exhibits the lowest $E_r$. At the same time, $Ca_2Fe_2O_5$ shows a significant decrease in $E_r$ with an increasing mixing ratio. For Cu, $CaFe_2O_4$ at a 5 % mixing ratio exhibited the smallest $E_r$, and $Ca_2Fe_2O_5$ increased and then decreased, with the lowest at 20 %. The $E_r$ value of Mn was lowest at a 3 % mixing rate of $CaFe_2O_4$, and the increase in adsorbent was less than that of other mixing rates. The change in $Ca_2Fe_2O_5$ was also small, with the lowest value at a mixing rate of 20 %. Ni's fixation rate was effectively improved by adding two calcium-iron type adsorbents. The $E_r$ of $CaFe_2O_4$ decreased significantly with the increase in the mixing ratio. The $E_r$ of $Ca_2Fe_2O_5$ first reduced and then increased, and it was the smallest at 10 % mixing ratio. The $E_r$ value of Pb at a 3 % mixing ratio increased slightly, which agrees with the analysis of CE. The toxicity of Zn is not high and increases and then decreases with the addition of $CaFe_2O_4$, and $Ca_2Fe_2O_5$ reaches the minimum at a 20 % mixing ratio.

Since adsorbents have selective adsorption of different types of heavy metals, a comprehensive index is needed to select the adsorption effect of adsorbents. This study will compare them by risk index. The $R_I$ of $CaFe_2O_4$ decreases with the increase of mixing ratio and reaches its minimum at 20 %, a reduction of about 58 % compared with the case of no added adsorbent. In contrast, $Ca_2Fe_2O_5$ reaches its minimum at a 5 % mixing ratio, which is reduced by about 35 % compared to the case without adding adsorbent. In addition, a side-by-side comparison of the two calcium-iron type adsorbents at the same mixing ratio showed that $CaFe_2O_4$ had a smaller $R_I$ value than $Ca_2Fe_2O_5$.

## 4. Conclusions

In this study, $CaFe_2O_4$ and $Ca_2Fe_2O_5$ were utilized to reduce the heavy metal elements (Cr, Cu, Mn, Ni, Pb, Zn) from entering the atmosphere and damaging the environment. Simulated thermal adsorption experiments were carried out using a tube furnace and Factsage to study the effect and mechanism of adsorption of heavy metals from coal and coconut shells by adsorbents. Meanwhile, two calculation methods, CE and Δ, were used to pool the ecological risks of heavy metals and comprehensively evaluate the effects of two calcium-iron type adsorbents.

1. $CaFe_2O_4$ and $Ca_2Fe_2O_5$ showed fixation effects on heavy metals at 900 °C under different mixing ratios by combining CE and Δ methods. Regarding the net fixation efficiency of heavy metals, the increase in the mixing ratio had a more significant effect on $CaFe_2O_4$. The results showed that the optimal fixation effect of $CaFe_2O_4$ with different mixing ratios at 900 °C was increased by 27.75 %, 14.27 %, 10.51 %, 46.14 %, 17.69 %, 10.66 %, and $Ca_2Fe_2O_5$ was increased by 36.58 %, 27.14 %, 4.99 %, 25.89 %, 15.88 %, and 13.24 %.
2. Integration of ecological risk considerations for heavy metals, a side-by-side comparison of the two calcium-iron type adsorbents at the same mixing ratio showed that $CaFe_2O_4$ had a smaller $R_I$ value than $Ca_2Fe_2O_5$. This implies that $CaFe_2O_4$ has better performance compared to $Ca_2Fe_2O_5$.

## CRediT authorship contribution statement

**Zi You:** Writing – original draft, Methodology, Investigation. **Chunxiang Chen:** Writing – review & editing, Resources, Methodology. **Jinxi Dong:** Writing – review & editing, Supervision. **Wenchang Yue:** Writing – review & editing, Supervision, Resources. **Xiaoqian Ma:** Writing – review & editing, Methodology, Conceptualization. **Zhaosheng Yu:** Writing – review & editing, Investigation, Funding acquisition.

## Declaration of Competing Interest

The authors declare that they have no known competing financial interests or personal relationships that could have appeared to influence

Table 4
Potential ecological risk factors and risk indices for individuals before and after the addition of two calcium-iron type adsorbents.

| Experimental parameters | | $E_r$ | | | | | | $R_I$ |
|---|---|---|---|---|---|---|---|---|
| Adsorbent | mixing ratio | Cr | Cu | Mn | Ni | Pb | Zn | |
| None | - | 2.29E+04 | 2.30E+04 | 1.21E+04 | 3.28E+05 | 1.02E+04 | 2.94E+03 | 3.99E+05 |
| $CaFe_2O_4$ | 3 % | 1.57E+04 | 2.09E+04 | 8.87E+03 | 2.09E+05 | 1.05E+04 | 2.58E+03 | 2.68E+05 |
| | 5 % | 1.71E+04 | 1.74E+04 | 1.21E+04 | 1.66E+05 | 8.30E+03 | 2.64E+03 | 2.24E+05 |
| | 10 % | 1.36E+04 | 1.82E+04 | 1.10E+04 | 1.16E+05 | 8.40E+03 | 2.72E+03 | 1.70E+05 |
| | 20 % | 2.07E+04 | 1.94E+04 | 1.11E+04 | 1.06E+05 | 7.51E+03 | 2.57E+03 | 1.67E+05 |
| $Ca_2Fe_2O_5$ | 3 % | 1.74E+04 | 1.70E+04 | 1.11E+04 | 2.53E+05 | 1.04E+04 | 2.75E+03 | 3.12E+05 |
| | 5 % | 1.63E+04 | 1.81E+04 | 1.15E+04 | 2.03E+05 | 7.79E+03 | 2.73E+03 | 2.60E+05 |
| | 10 % | 1.49E+04 | 1.74E+04 | 1.13E+04 | 2.23E+05 | 1.03E+04 | 2.77E+03 | 2.79E+05 |
| | 20 % | 1.06E+04 | 1.24E+04 | 1.06E+04 | 2.99E+05 | 1.08E+04 | 2.49E+03 | 3.46E+05 |

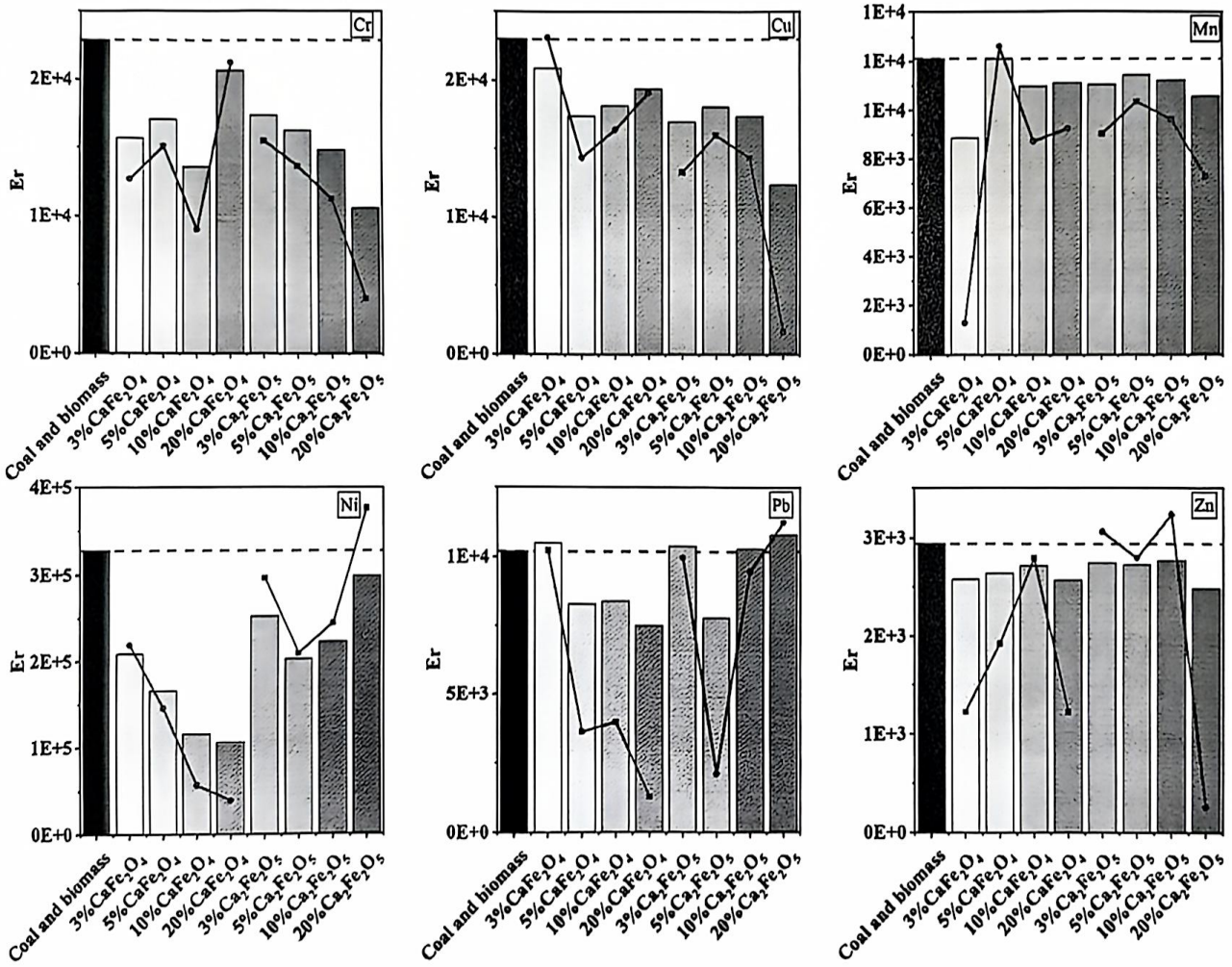


Fig. 5. Er of heavy metals by two calcium-iron type adsorbents.

the work reported in this paper.

## Data availability

Data will be made available on request.

## Acknowledgments

This work was supported by the Guangxi Key Research and Development Natural Science Foundation (GUIKEAB22035033) and the Fundamental Research Funds for the Central Universities (2022ZFJH04).

## Appendix A. Supporting information

Supplementary data associated with this article can be found in the online version at doi:10.1016/j.indcrop.2024.119291.

## References

Benallal, S., Boumaza, S., Brahimi, R., et al., 2022. Electrochemical characterization of the brownmillerite Ca2Fe2O5+δ synthesized by citrate sol–gel method. Application to photocatalytic H2-production. J. Solid State Electrochem. [J. ] 26, 1541–1547.
Bloesser, A., Timm, J., Kurz, H., et al., 2020. A novel synthesis yielding macroporous CaFe2O4 sponges for solar energy conversion. Sol. RRL 4, 1900570.

Bo, X., Wang, D., Wan, X.G., 2021. Calculated magnetic exchange interactions in brownmillerite Ca2Fe2O5. Phys. Lett. A 394, 127202.
Bouatam, I., Lahmar, H., Dounfer, S., et al., 2022. Sol. Photo Rose Bengal Water Spine CaFe2O4. Opt. 266, 169635.
Chen, L., Liao, Y., Ma, X., 2019. Heavy metals volatilization characteristics and risk evaluation of co-combusted municipal solid wastes and sewage sludge without and with calcium-based sorbents. Ecotoxicol. Environ. Saf. 182, 109370.109371-109370.109310.
Feng, Y., Wang, N., Guo, X., et al., 2020. Reaction mechanism of Ca2Fe2O5 oxygen carrier with CO in chemical looping hydrogen production. Appl. Surf. Sci. 534, 147583.
Gong, Z., Liu, L., Zhang, H., et al., 2021. Study on migration characteristics of heavy metals during the oil sludge incineration with CaO additive. Chem. Eng. Res. Des. 166, 55–66.
Hakanson L. 1980. An Ecological Risk Index for Aquatic Pollution Control – A Sedimentological Approach.
Hu, H.-Y., Liu, H., Shen, W.-Q., et al., 2013. Comparison of CaO's effect on the fate of heavy metals during thermal treatment of two typical types of MSWI fly ashes in China. Chemosphere 93, 590–596.
Hu, Y., You, M., Liu, G., et al., 2021. Characteristics and potential ecological risks of heavy metal pollution in surface soil around coal-fired power plant. Environ. Earth Sci. 80, 566.
Huang, L., Fan, Z., Li, X., et al., 2021. Facile synthesis of CaFe2O4 nanocubes for formaldehyde sensor. Mater. Lett. 288, 129351.
Jagodzińska, K., Mroczek, K., Nowińska, K., et al., 2019. The impact of additives on the retention of heavy metals in the bottom ash during RDF incineration. Energy 183, 854–868.
Ke, C., Ma, X., Tang, Y., et al., 2019. Effects of natural and modified calcium-based sorbents on heavy metals of food waste under oxy-fuel combustion. Bioresour. Technol. 271, 251–257.
Kenfoud, H., Nasrallah, N., Baaloudj, O., et al., 2020. Photocatalytic reduction of Cr(VI) onto the spinel CaFe2O4 nanoparticles. Optik 223, 165610.
Lai, X., Zhong, Z., Xue, Z., et al., 2020. Experimental study on enrichment of heavy metals by intercalation-exfoliation modified kaolin during coal combustion. Environ. Technol. 41, 3464–3472.
Li, C., Han, Q., Zhu, T., et al., 2020. Radical-dominated reaction of CO–NO on a CaFe 2 O 4 surface in sintering flue gas recirculation. RSC Adv. 10, 23491–23497.
Linak, W.P., Srivastava, R.K., Wendt, J.O.L., 1995. Sorbent capture of nickel, lead, and cadmium in a laboratory swirl flame incinerator. Combust. Flame 100, 241–250.
Luo, J.-Z., Sheng, B.-X., Shi, Q.-Q., 2020. A review on the migration and transformation of heavy metals influence by alkali/alkaline earth metals during combustion. J. Fuel Chem. Technol. 48, 1318–1326.
Manohar, A., Vijayakanth, V., Mameda, N., et al., 2024. Revolutionizing nanoscience: Exploring the multifaceted applications and cutting-edge advancements in spinel CaFe2O4 nanoparticles – A review. Inorg. Chem. Commun. 161, 111999.
Miller, D.D., Siriwardane, R., 2018. CaFe2O4 oxygen carrier characterization during the partial oxidation of coal in the chemical looping gasification application. Appl. Energy 224, 708–716.
Munawer, M.E., 2018. Human health and environmental impacts of coal combustion and post-combustion wastes. J. Sustain. Min. 17, 87–96.
Obolrien, B.O., Thulari, V., North, B.C., 2016. Enrichment of trace elements in bottom ash from coal oxy-combustion: effect of coal types. Appl. Energy 177, 81–86.
Qomaruddin, Casals, O., Sutka, A., et al., 2020. Visible light-driven p-type semiconductor gas sensors based on CaFe2O4 nanoparticles. Sensors 20, 850.
Ran, C., Liu, Y., Siddiqui, A.R., et al., 2019. Pyrolysis of textile dyeing sludge in fluidized bed: analysis of products, and migration and distribution of heavy metals. J. Clean. Prod. 241, 118308.
Saiknew, T., Supudommak, P., Meksur, L., et al., 2012. Emission of NOx and N2O from co-combustion of coal and biomasses in CFB combustor. Int. J. Greenh. Gas. Control 10, 26–32.
Scotto, M.V., Uberoi, M., Peterson, T.W., et al., 1994. Metal capture by sorbents in combustion processes. Fuel Process. Technol. 39, 357–372.
Singh, M., Thind, P.S., John, S., 2018. Health risk assessment of the workers exposed to the heavy metals in e-waste recycling sites of Chandigarh and Ludhiana, Punjab, India. Chemosphere 203, 426–433.
Ueda H., Skoropata E., Plamonteze C., et al. 2022. Unusual ferrimagnetism in ${\mathrm{Ca}{\mathrm{Fe}}_{2}\mathrm{O}}_{4}$. Physical Review Materials [J], 6: 124405.
Wang, W., Chen, H., Wang, A., 2007. Adsorption characteristics of Cd(II) from aqueous solution onto activated palygorskite. Sep. Purif. Technol. 55, 157–164.
Wasielewski, R., Glód, K., Lasek, J., 2021. Industrial tests of co-combustion of alternative fuel with hard coal in a stoker boiler. J. Air Waste Manag. Assoc. 71, 339–347.
Xue, Z., Dong, L., Zhong, Z., et al., 2021. Capture effect of Pb, Zn, Cd and Cr by intercalation-exfoliation modified montmorillonite during coal combustion. Fuel 290, 119980.
Yang, Y., Zhong, Z., Li, J., et al., 2023a. Low-consumption with efficient capture and characteristics of heavy metals from coal combustion by modified kaolin: experimental and simulation studies. Fuel 332, 126094.
Yang, Y., Zhong, Z., Li, J., et al., 2023b. Experimental and theoretical-based study of heavy metal capture by modified silica-alumina-based materials during thermal conversion of coal at high temperature combustion. Appl. Energy 351, 121829.
Yao, H., Mkilaha, I.S.N., Naruse, I., 2004. Screening of sorbents and capture of lead and cadmium compounds during sewage sludge combustion. Fuel 83, 1001–1007.
Yao, H., Naruse, I., 2009. Using sorbents to control heavy metals and particulate matter emission during solid fuel combustion. Particuology 7, 477–482.
Zhang, K., Hong, W., Gao, P., et al., 2020. Orthorhombic CaFe2O4 microrod anode for lithium-ion battery - ScienceDirect. Int. J. Hydrog. Energy [J. ] 45, 22160–22165.
Zhang, Z., Huang, Y., Zhu, Z., et al., 2022. Effect of CaO and montmorillonite additive on heavy metals behavior and environmental risk during sludge combustion. Environ. Pollut. 312, 120024.
Zhao, Y., Yang, J., Ma, S., et al., 2018. Emission controls of mercury and other trace elements during coal combustion in China: a review. Int. Geol. Rev. 60, 638–670.
Zheng W., Ma X., Tang Y., et al. 2017. Heavy metal control by natural and modified limestone during wood sawdust combustion in a CO2/O2 atmosphere. Energy & Fuels [J].
Zhu, Z., Huang, Y., Yu, M., et al., 2024. Effect of NaCl on the migration of heavy metals during the non-isothermal and isothermal combustion of sludge: Static and dynamic analyses. J. Hazard. Mater. 468, 133699.
Zhuang, S., Lu, X., 2020. Environmental Risk Evaluation and Source Identification of Heavy Metal(loid)s in Agricultural Soil of Shangdan Valley, Northwest China. Sustainability 12, 5806.